# Micropores in Crystalline Dipeptides as Seen from the Crystal Structure, He Pycnometry, and 129 Xe NMR Spectroscopy

**ARTICLE** *in* JOURNAL OF THE AMERICAN CHEMICAL SOCIETY · JUNE 2006

Impact Factor: 12.11 · DOI: 10.1021/ja060474j · Source: PubMed



**4 AUTHORS**, INCLUDING:

Dmitriy Soldatov
University of Guelph
**103** PUBLICATIONS **1,821** CITATIONS
SEE PROFILE

John A. Ripmeester
National Research Council Canada
**713** PUBLICATIONS **15,518** CITATIONS
SEE PROFILE

J|A|C|S
ARTICLES
Published on Web 04/28/2006

# Micropores in Crystalline Dipeptides as Seen from the Crystal Structure, He Pycnometry, and $^{129}$Xe NMR Spectroscopy

Dmitriy V. Soldatov,*[,†,‡] Igor L. Moudrakovski,[‡] Eugeny V. Grachev,[†] and John A. Ripmeester*[,‡]

*Contribution from the Nikolaev Institute of Inorganic Chemistry, Russian Academy of Sciences, Novosibirsk, Russia, and Steacie Institute for Molecular Sciences, National Research Council, Ottawa, Canada*

Received January 20, 2006; E-mail: soldatov@che.nsk.su; John.Ripmeester@nrc.ca

***Abstract:*** Eight crystalline dipeptides were studied: AV (Ala-Val), VA (Val-Ala), AI (Ala-Ile), VV (Val-Val), IA (Ile-Ala), IV (Ile-Val), VI (Val-Ile), and LS (Leu-Ser) (all LL isomers). The first seven form an isostructural series (space group $P6_1$), whereas LS has a different structure ($P6_5$). All structures display H-bonded tubular assemblies of the dipeptide molecules resulting in open ultramicropores in the form of isolated one-dimensional (1D) channels. The total porosity of the materials ranges from 4 to 12% (micropore volume from 0.04 to 0.12 cm$^3$/g). Calculations based on the crystal structures, He pycnometry, and solid-state $^{129}$Xe NMR methods were used to obtain a comprehensive description of the geometry and properties of the micropores. The following order was established for the channel diameter: AV > VA > AI > VV > IA > IV > VI, with >5 Å for AV and <4 Å for VI; LS is close to AI. The observed sorption behavior cannot be described adequately based on the crystal structure and can only be understood if one takes into account the dynamics of the host matrix. The pores are chiral, with the center of the channel describing a right-handed helix (left-handed for LS). The following order was established for the channel helicity: VA > IA > IV > AV ≈ AI ≈ VV > VI > LS, with a helix diameter of ∼2 Å for VA, IA, and IV and ∼1 Å or less for the remaining dipeptides. A comparison of the dipeptides studied with other supramolecular materials is given and the potential for applications is discussed.

## Introduction

The research on, and development of, organically based microporous materials has become one of major areas in material science, supramolecular chemistry, and crystal engineering.[1,2] These materials are a challenge to practically useful inorganic sorbents (clays, zeolites, etc.) because of a number of important distinctions and advantages. Recently studied organically based micropores that may be incorporated in bulk materials indicate wide diversity and great potential for variation, high flexibility, and resemblance to biological patterns and display various compositions, structures, and functions.[3−11]

The geometry of the free void space is a primary characteristic of micropores in solids. In most cases, the included species (guest) and the micropore (host) are linked by noncovalent, frequently by only van der Waals, interactions. Therefore, total capacity, selectivity toward certain guests, kinetics of inclusion, and other important properties of micropores may be understood and predicted from a knowledge of the micropore geometry. In the literature, a fair number of examples describing the geometry of molecular-scale empty space in solids is given[12−24] (and illustrated for inorganic,[15,16] metal-organic,[17−19] organic,[8,20] and

[†] Russian Academy of Sciences.
[‡] National Research Council.

(1) Kitagawa, S.; Kitaura, R.; Noro, S. *Angew. Chem., Int. Ed.* **2004**, *43*, 2334−2375.
(2) Soldatov, D. V.; Ripmeester, J. A. Organic Zeolites. In *Nanoporous Materials IV*; Sayari A., Jaroniec M., Eds.; Elsevier: Amsterdam, 2005; pp 37−54.
(3) Mitchell, K. D. D.; Fyles, T. M. Ion Channels and Their Models. In *Encyclopedia of Supramolecular Chemistry*; Atwood, J. L., Steed, J. W., Eds.; Marcel Dekker: New York, 2004; pp 742−746.
(4) Malek, K.; Odijk, T.; Coppens, M. O. *ChemPhysChem* **2004**, *5*, 1596−1599, and refs 1−5 therein.
(5) Kitaura, R.; Onoyama, G.; Sakamoto, H.; Matsuda, R.; Noro, S.; Kitagawa, S. *Angew. Chem., Int. Ed.* **2004**, *43*, 2684−2687, and refs 3, 6 therein.
(6) Zyryanov, G. V.; Rudkevich, D. M. *J. Am. Chem. Soc.* **2004**, *126*, 4264−4270, and ref 5 therein.
(7) Organo, V. G.; Leontiev, A. V.; Sgarlata, V.; Dias, H. V. R.; Rudkevich, D. M. *Angew. Chem., Int. Ed.* **2005**, *44*, 3043−3047, and refs 3, 4 therein.
(8) Tedesco, C.; Immediata, I.; Gregoli, L.; Vitagliano, L.; Immirzi, A.; Neri, P. *CrystEngComm* **2005**, *7*, 449−453.
(9) Gorteau, V.; Bollot, G.; Mareda, J.; Pasini, D.; Tran, D. H.; Lazar, A. N.; Coleman, A. W.; Sakai, N.; Matile, S. *Bioorg. Med. Chem.* **2005**, *13*, 5171−5180, and refs 1−14 therein.
(10) Hector, R. C.; Gin, M. S. *Supramol. Chem.* **2005**, *17*, 129−134.
(11) Percec, V.; Dulcey, A.; Peterca, M.; Ilies, M.; Miura, Y.; Edlund, U.; Heiney, P. A. *Aust. J. Chem.* **2005**, *58*, 472−482.
(12) Richards, F. M. *Methods Enzymol.* **1985**, *115*, 440−464.
(13) Grachev, E. V.; Dyadin Y. A.; Lipkowski, J. *J. Struct. Chem.* **1995**, *36*, 876−879.
(14) George, A. R.; Harris, K. H. M. *J. Mol. Graphics* **1995**, *13*, 138−141.
(15) Moudrakovski, I. L.; Ratcliffe, C. I.; Ripmeester, J. A. *Appl. Magn. Res.* **1996**, *10*, 559−574.
(16) Khan, M. I.; Meyer, L. M.; Haushalter, R. C.; Schweitzer, A. L.; Zubieta, J.; Dye, J. L. *Chem. Mater.* **1996**, *8*, 43−53.
(17) Lipkowski, J.; Soldatov, D. V. *J. Inclusion Phenom.* **1994**, *18*, 317−329.
(18) Soldatov, D. V.; Ripmeester, J. A.; Shergina, S. I.; Sokolov, I. E.; Zanina, A. S.; Gromilov, S. A.; Dyadin, Yu. A. *J. Am. Chem. Soc.* **1999**, *121*, 4179−4188.
(19) Soldatov, D. V.; Grachev, E. V.; Ripmeester, J. A. *Cryst. Growth Des.* **2002**, *2*, 401−408.
(20) Brunet, P.; Demers, E.; Maris, T.; Enright, G. D.; Wuest, J. D. *Angew. Chem., Int. Ed.* **2003**, *42*, 5303−5306.
(21) Margolin, A. L.; Navia, M. A. *Angew. Chem., Int. Ed.* **2001**, *40*, 2204−2222.

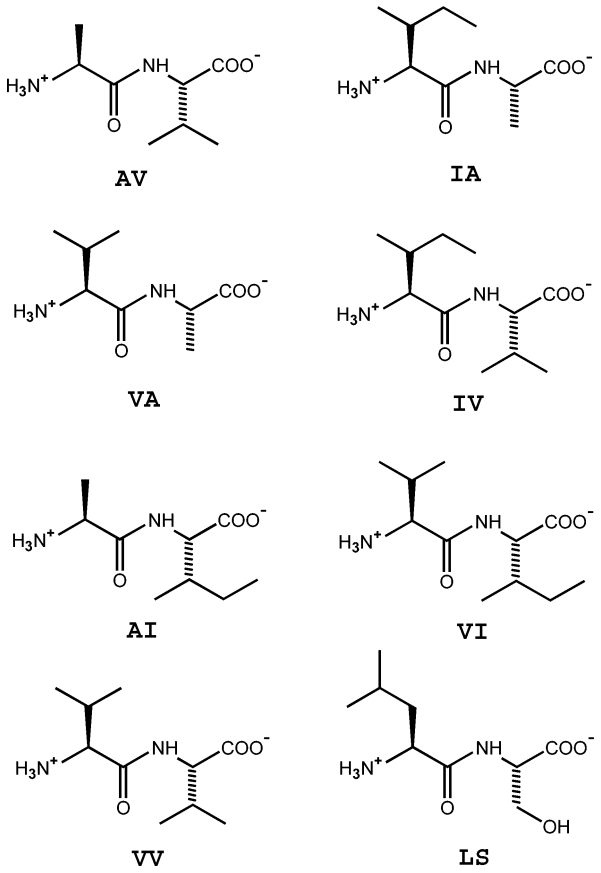


***Figure 1.*** Dipeptides studied.

peptide/protein[21−24] materials). Remarkably, the number of descriptive methods still in use is quite impressive, indicating the complicacy of the problem. In most cases, the description is based on a single method only and is not supported by independent experimental evidence. In particular, a number of unrealistic values for porosity is based on crystallographic data.

This study is devoted to the description of empty micropore space in a series of eight crystalline dipeptides (Figure 1). The porous space, in the form of one-dimensional (1D) channels, is observed in the low-temperature crystal structures of the compounds: AV (150 K);[25] VA (120 K);[26] AI, VV (150 K);[27] IA, IV, VI (105 K);[27] LS (105 K).[28] Direct sorption experiments conducted for bulk AV and VA indicated that more than 10% of the materials' volume is readily and reversibly accessible to gases (He, Xe)[22,29] that allowed us to qualify these materials as "biozeolites", a group of organically based zeolite mimics.[2] Here, we report the investigation of micropore geometry in eight crystalline dipeptides with three independent methods. Room-temperature single-crystal XRD studies were done to allow a comparison of crystal structures throughout the series and to establish consistency with the other two methods. He pycnometry[30−32] was used to estimate the actual space in the material accessible to the He gas. Finally, solid-state $^{129}$Xe NMR with optically polarized and highly dilute xenon gas was applied to probe the micropores directly.[29,33−37]

## Experimental Section

**Preparations.** All dipeptides were obtained from Bachem. Powdered samples for He pycnometry and $^{129}$Xe NMR were prepared by grinding as-received chemicals (except LS) followed by drying (60 °C, several hours) to remove moisture from the pores. LS had to be recrystallized prior to the preparations by adding an excess of acetonitrile to a concentrated aqueous solution of the dipeptide. A cotton-like crystalline product was then separated, air-dried, and treated in an oven (60 °C, 1 day) to remove acetonitrile from the pores. As attested by powder XRD, each sample comprised only a single phase that was identical with that found in the corresponding single-crystal XRD experiment.

The single crystals of the dipeptides for XRD studies were grown from aqueous solutions without using templates (except LS) as described in a previous work for AV and VA.[22] The crystals were dried in an oven (60 °C, 1 day) to remove moisture from the pores and were studied in an atmosphere of nitrogen. The single crystal of LS was grown as described by Görbitz et al.[28] and dried in an oven (100 °C, 2 days) to remove guest acetonitrile.

**XRD Studies.** Powder XRD patterns were recorded on a Rigaku Geigerflex diffractometer (Co $K_\alpha$ radiation, $\lambda = 1.7902$ Å) in the 5−30° $2\theta$ range. Single crystals were studied on a Bruker SMART CCD X-ray diffractometer (Mo $K_\alpha$ radiation, $\lambda = 0.71073$ Å, graphite monochromator). The data collections were set up to cover a complete Ewald sphere to ensure high redundancy, to a max $2\theta \approx 60°$. The unit cell parameters were refined using entire data sets.

The structures were solved by direct methods using SIR92.[38] The structural refinement using the SHELXTL package[39] was performed on $F^2$ and applied to all data with positive intensities. Non-hydrogen atoms were refined anisotropically, with the exception of atoms in a minor orientation (9.6(5) %) of the isopropyl residue of valyl in VI. The greatest electron density maxima found in the channels were (the greatest max for each structure is given in brackets for comparison): AI, 0.07 (0.24); VV, 0.06 (0.18); IA, 0.09 (0.17); IV, 0.06 (0.18); VI, 0.10 (0.21); LS, 0.17 (0.23) e/Å$^3$. The molecular geometry and intermolecular contacts were analyzed with SHELXTL[39] and PARST.[40] Essential crystal data and experimental parameters are given in Table 1. Further experimental details and full lists of results were deposited with CCDC (deposition numbers are listed in Table 1) and are given in the Supporting Information.

**Analysis of Crystal Packing and Empty Space.** Room-temperature single-crystal XRD results reported previously (AV, VA)[22] and derived

(22) Soldatov, D. V.; Moudrakovski, I. L.; Ripmeester, J. A. *Angew. Chem., Int. Ed.* **2004**, *43*, 6308−6311.
(23) Malek, K.; Odijk, T.; Coppens, M. O. *Nanotechnology* **2005**, *16*, S522−S530.
(24) Smith, R. D.; Hu, L.; Falkner, J. A.; Benson, M. L.; Nerothin, J. P.; Carlson, H. A. *J. Mol. Graphics Modell.* **2006**, *24*, 414−425, and refs therein.
(25) Görbitz, C. H. *Acta Crystallogr., Sect. B: Struct. Sci.* **2002**, *58*, 849−854.
(26) Görbitz, C. H.; Gunderson, E. *Acta Crystallogr., Sect. C: Cryst. Struct. Commun.* **1996**, *C52*, 1764−1767.
(27) Görbitz, C. H. *New J. Chem.* **2003**, *27*, 1789−1793.
(28) Görbitz, C. H.; Nilsen, M.; Szeto, K.; Tangen, L. W. *Chem. Commun.* **2005**, 4288−4290.
(29) Moudrakovski, I. L.; Soldatov, D. V.; Ripmeester, J. A.; Sears, D. N.; Jameson, C. J. *Proc. Natl. Acad. Sci. U.S.A.* **2004**, *101*, 17924−17929.
(30) De Boer, J. H.; Steggerda, J. J. *Proc. Koninkl. Nederl. Akad. Weterschappen Amsterdam, Ser. B* **1958**, *61*, 317−323.
(31) Sircar, S. *Ind. Eng. Chem. Res.* **1999**, *38*, 3670−3682.
(32) Tamari, S. *Meas. Sci. Technol.* **2004**, *15*, 549−558.
(33) Moudrakovski, I. L.; Nossov, A.; Lang, S.; Breeze, S. R.; Ratcliffe, C. I.; Simard, B.; Santyr, G.; Ripmeester, J. A. *Chem. Mater.* **2000**, *12*, 1181−1183.
(34) Moudrakovski, I.; Lang, S.; Ratcliffe, C. I.; Santyr, G.; Ripmeester, J. *J. Magn. Res.* **2000**, *144*, 372−377.
(35) Nossov, A. V.; Soldatov, D. V.; Ripmeester, J. A. *J. Am. Chem. Soc.* **2001**, *123*, 3563−3568.
(36) Moudrakovski, I. L.; Nossov, A. V.; Terskikh, V. V.; Lang, S.; Brouwer, E. B.; Soldatov, D. V.; Ratcliffe, C. I.; Ripmeester, J. A. Applications of Hyperpolarized $^{129}$Xe NMR Spectroscopy to the Study of Materials. In *Magnetic Resonance in Colloid and Interface Science*; Fraissard, J., Lapina, O., Eds.; Kluwer: Amsterdam, 2002; pp 115−122.
(37) Sears, D. N.; Demko, B. A.; Ooms, K. J.; Wasylishen, R. E.; Huang, Y. *Chem. Mater.* **2005**, *17*, 5481−5488.
(38) Altomare, A.; Cascarano, G.; Giacovazzo, C.; Gualardi, A. *J. Appl. Crystallogr.* **1993**, *26*, 343−350.
(39) Sheldrick, G. M. *SHELXTL PC*, Ver. 4.1. An Integrated System for Solving, Refining and Displaying Crystal Structure from Diffration Data; Siemens Analytical X-ray Instruments, Inc.: Madison, WI, 1990.
(40) Nardelli, M. *J. Appl. Crystallogr.* **1995**, *28*, 659.

***Table 1.*** Room Temperature Crystal Structure Data and Selected Parameters of the XRD Analysis for the Dipeptides Studied

| compound | AV | VA | AI | VV | IA | IV | VI | LS |
|---|---|---|---|---|---|---|---|---|
| empirical formula | $C_8H_{16}N_2O_3$ | $C_8H_{16}N_2O_3$ | $C_9H_{18}N_2O_3$ | $C_{10}H_{20}N_2O_3$ | $C_9H_{18}N_2O_3$ | $C_{11}H_{22}N_2O_3$ | $C_{11}H_{22}N_2O_3$ | $C_9H_{18}N_2O_4$ |
| molecular mass | 188.2 | 188.2 | 202.3 | 216.3 | 202.3 | 230.3 | 230.3 | 218.3 |
| cryst. system, sp. gr. | hex., $P6_1$ | hex., $P6_1$ | hex., $P6_1$ | hex., $P6_1$ | hex., $P6_1$ | hex., $P6_1$ | hex., $P6_1$ | hex., $P6_5$ |
| *a*, Å | 14.462(2) | 14.461(2) | 14.261(2) | 14.573(2) | 14.481(2) | 14.871(2) | 14.774(2) | 18.138(2) |
| *c*, Å | 10.027(1) | 10.083(1) | 10.221(1) | 10.354(1) | 10.037(1) | 10.305(1) | 10.319(1) | 6.163(1) |
| *V*, Å$^3$ | 1816.2(4) | 1826.1(4) | 1800.2(4) | 1904.3(4) | 1822.8(4) | 1973.6(4) | 1950.6(4) | 1755.9(4) |
| Z | 6 | 6 | 6 | 6 | 6 | 6 | 6 | 6 |
| calcd density, g cm$^{-3}$ | 1.033 | 1.027 | 1.119 | 1.132 | 1.106 | 1.163 | 1.176 | 1.238 |
| final *R1* ($I > 2\sigma(I)$) | 0.048 | 0.057 | 0.034 | 0.030 | 0.037 | 0.030 | 0.031 | 0.029 |
| data/param. ratio | 15.4 | 16.0 | 22.0 | 21.6 | 21.8 | 21.3 | 19.6 | 20.5 |
| disorder | Val, $(CH_3)_2$ 70/21/9% | − | − | − | − | − | Val, $C(CH_3)_2$ 90/10% | − |
| peak/hole, e Å$^{-3}$ | +0.17/−0.15 | +0.15/−0.14 | +0.24/−0.13 | +0.18/−0.12 | +0.17/−0.14 | +0.18/−0.14 | +0.21/−0.18 | +0.23/−0.11 |
| CCDC deposition no | − | − | 290257 | 290258 | 290259 | 290260 | 290261 | 290262 |
| reference | a | a | this work | this work | this work | this work | this work | this work |

[a] Reference 22.

in this work (all other dipeptides) were corrected slightly: hydrogen atoms were reattached at 1.08 Å for C−H bonds and 1.00 Å for N−H and O−H bonds; only major orientations of disordered fragments were left for AV (70%) and VI (90%). The following system of van der Waals radii was applied: C, 1.71; H, 1.16; N, 1.50; O, 1.29;[41] He, 1.40; Xe, 2.16 Å.[42] Packing coefficients were calculated using the CLAT program package.[13] The pore shapes were drawn with help of ATOMS.[43] Precise calculation of pore geometries was carried out by inscribing a set of ∼500 spheres per translation (∼300 for LS) according to the following procedure. On each level, separated from other levels by 0.02 Å along the *c* axis (along the channel), a sphere of maximal possible diameter was inscribed that touched but did not overlap the peptide atoms drawn at their van der Waals dimensions. The diameter of a sphere on each level was taken as the diameter of the channel on this level, and the center of the sphere was taken as the center of the channel on this level.

**He Pycnometry.** Measurements were run on an AccuPyc 1330 gas pycnometer (Micromeritics) at 26 ± 1 °C. The accuracy of the density measurement was tested with ground NaCl to give an average of three independent measurements of 2.163(2) g/cm$^3$ (room-temperature theoretical density 2.165 g/cm$^3$). Each sample was measured several times (10 runs in each determination) to achieve stable results. The sample mass in the range of 100−150 mg and the equilibration rate of 0.003 psig/min were found to be appropriate as a 2-fold reduction of the mass and 3-fold reduction of the rate did not alter the results.

The total porosity of the materials studied ($P^{(He)}$, %) was calculated as the space fraction in a sample accessible to the helium gas: $P^{(He)} = 100(V_{empty}/V_{u.cell}) = 100(1 - d_{calc}/d^{(He)})$, where $V_{empty}$ = volume of unit cell accessible to He, $V_{u.cell}$ = volume of the unit cell, $d_{calc}$ = density calculated from XRD data (room temperature), $d^{(He)}$ = density from He pycnometry measurement (density of the host body framework, "skeletal density"). The average diameter of the channel as estimated from He pycnometry ($D^{(He)}$) was derived from $D^{(He)} = 2(V_{empty}/(c\pi))^{1/2}$, $V_{empty} = (P^{(He)} V_{u.cell})/100$, where *c* is the translation period of the channel equal to the unit cell parameter (Table 2).

**$^{129}$Xe NMR.** All $^{129}$Xe NMR measurements were performed on a Bruker DSX-400 instrument operating at 110.8 MHz (magnetic field of 9.4 T) using a continuous flow of hyperpolarized (CF HP) Xe. A modified Bruker 7-mm BL MAS probe similar to that used in refs 33 and 35 was employed for all experiments. The continuous-flow polarizer for production of HP Xe was of a design similar to that reported in ref 34 and operated with an 80 W diode laser from Coherent (effective wavelength and line width were 795 and 1.2 nm, respectively). A xenon−helium−nitrogen mixture with a volume composition of 1:98:1% was used in all CF HP experiments. The flow rate was monitored with a Vacuum General flow controller (Model 80-4) and kept constant in the range of 80−100 cm$^3$/min (gas flow normalized to standard conditions). In the CF HP experiments a flow of HP xenon was delivered directly into the coil region of an NMR probe through 1.5 mm ID plastic tubing. All $^{129}$Xe NMR measurements were performed at 295 K. The reported $^{129}$Xe NMR chemical shifts were referenced to xenon gas extrapolated to zero pressure. The experimental static powder patterns were fitted using the DMFIT NMR simulation package.[44]

***Table 2.*** Results of He Pycnometry Experiments

| compound | $d_{calc}$, g/cm$^3$ | $d^{(He)}$, g/cm$^3$ | $P^{(He)}$, % | $D^{(He)}$, Å |
|---|---|---|---|---|
| AV | 1.033 | 1.180(2) | 12.5(2) | 5.36(8) |
| VA | 1.027 | 1.157(2) | 11.2(2) | 5.08(8) |
| AI | 1.119 | 1.221(2) | 8.3(2) | 4.3(1) |
| VV | 1.132 | 1.216(2) | 6.9(2) | 4.0(1) |
| IA | 1.106 | 1.173(2) | 5.7(2) | 3.6(1) |
| IV | 1.163 | 1.221(2) | 4.8(2) | 3.4(1) |
| VI | 1.176 | 1.221(2) | 3.7(2) | 3.0(2) |
| LS | 1.238 | 1.304(3) | 5.1(3) | 4.3(2) |

## Results and Discussion

**Crystal Structures of the Dipeptides.** The eight dipeptide structures of this work fall into two groups (Table 1). Seven dipeptides whose molecules are composed of hydrophobic amino acids (Ala < Val < Ile) form an isostructural series (hexagonal, space group $P6_1$). The channel results from a spiral H-bonded assembly of the dipeptide molecules into a nanotube (Figure 2) aligned along the hexagonal axis of the structure. Each channel is formed 50% from one nanotube and 50% from six parallel adjacent nanotubes. The channels are one-dimensional and isolated from each other. The inner walls of the channels are formed by the hydrocarbon fragments of both residues of the dipeptide molecule and are essentially hydrophobic. The diameter of the nanotube equals the *a* parameter of the crystal structure and varies within 14.2−14.9 Å. The dimensions across the interior channel space are defined mostly by the size of hydrocarbon fragments, and these are discussed in a later section. The translation period varies from 10 to 10.4 Å and includes a 6-fold screw rotation.

LS forms a unique structure (hexagonal, space group $P6_5$). There is a somewhat similar H-bonding spiral assembly yielding

(41) Zefirov, Y. V.; Zorkii, P. M. *Zh. Strukt. Khim.* **1974**, *15*(1), 118−122.
(42) Bondi, A. *J. Phys. Chem.* **1964**, *68*, 441−451.
(43) Dowty, E. *ATOMS*, Ver. 5.0.6. Complete Program for Displaying Crystal Structures; Kingsport, TN, 1999.
(44) Massiot, D.; Fayon, F.; Capron, M.; King, I.; Le Calvé, S.; Alonso, B.; Durand, J.-O.; Bujoli, B.; Gan, Z.; Hoatson, G. *Magn. Reson. Chem.* **2002**, *40*, 70−76.

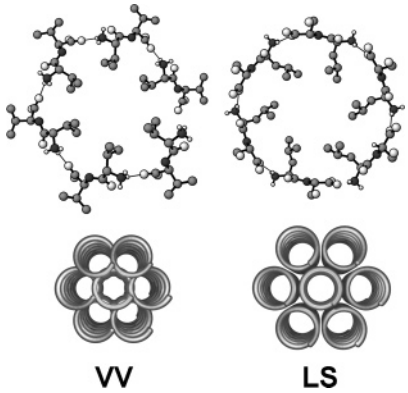


***Figure 2.*** Molecular assembly and packing in VV and LS. (Top) Spiral H-bonding assembly of molecules that forms a nanotube. Hydrogen atoms of amino groups only are shown; hydrogen bonds are designated with thin solid sticks. (Bottom) Schematic illustration of the packing of peptide nanotubes into the crystal structure.

***Table 3.*** Total Empty Space and Porosity in the Materials Studied

| | | | porosity, % | |
|---|---|---|---|---|
| compound | $k_{pack}$ | total empty space, % | $P^{(He)}$ | calculated |
| AV | 0.537(4) | 46.3 | 12.5(2) | 10.90 |
| VA | 0.537(4) | 46.3 | 11.2(2) | 9.68 |
| AI | 0.597(5) | 40.3 | 8.3(2) | 10.02 |
| VV | 0.616(4) | 38.4 | 6.9(2) | 8.23 |
| IA | 0.591(5) | 40.9 | 5.7(2) | 6.04 |
| IV | 0.644(5) | 35.6 | 4.8(2) | 6.25 |
| VI | 0.652(5) | 34.8 | 3.7(2) | 5.69 |
| LS | 0.633(6) | 36.7 | 5.1(3) | 5.08 |

a nanotube with ~15 Å diameter and 6.2 Å translation period. The 1D isolated channel is formed completely from a single nanotube, with inner walls paved by the hydrophobic fragment of leucyl (Figure 2). In contrast to the right-handed channel helicity of the other dipeptides, the channel in LS is left-handed. More details on the crystal structure of the dipeptides studied may be found in earlier work.[22,25−29]

**Experimental Porosity and Total Empty Space.** The total porosity of a material is a fraction of its volume freely accessible to guest (sorbate) species. The porosity is only a part of the total empty space in a material. For crystalline solids, the packing coefficients[45] typically range from 0.5 to 0.8, meaning that 20−50% of all space is empty. The comparison of total empty space and porosity (for He as guest) in the materials studied is given in Table 3.

The experimental porosity in the series ($P^{(He)}$) varies from 4 to 12% to give micropore volumes of 0.04−0.12 $cm^3/g$. For comparison, the following micropore volumes were found in zeolites: 0.12−0.36 $cm^3/g$ (zeolite A, zeolite X, zeolite L, chabazite, including their variations and modifications),[46a] 0.13 $cm^3/g$ (ZSM-5),[47] 0.15−0.34 $cm^3/g$ (NaY and its 5 modifications),[48] 0.10−0.16 $cm^3/g$ (BEA and its 10 modifications).[49] The micropore volume in a series of pillared clays was found to vary from 0.08 to 0.14 $cm^3/g$.[50]

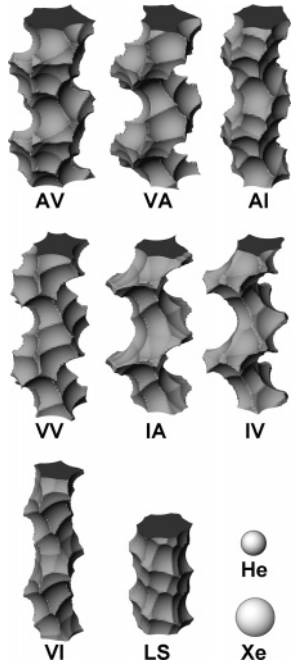


***Figure 3.*** Illustration of pore space in the materials studied. Two translation periods are shown in each case. The van der Waals outlines for He and Xe are given on the same scale for comparison.

The greatest porosity is observed for AV and VA; these dipeptides also have very low packing coefficients and may be expected to have more stable, dense polymorphic modifications. The empty space is most efficiently organized in these materials, contributing one-fourth to the pore system. The lowest porosity is observed for VI; this dipeptide has a relatively dense packing, implying it will be stable even in the absence of included guest species. Also, the empty space is more evenly distributed throughout the structure, and only a small fraction contributes to the pores.

**Calculated Porosity.** The calculated porosities are listed in Table 3. The calculation of porosity from crystal structure data is somewhat ambiguous. One problem is that the magnitude of porosity will naturally depend on the size and shape of the guest. In practice, the total porosity is expected to be similar for monatomic molecules of different diameter if the sieving effect is not too strong. Another problem is how to separate pore space from the total empty space in the crystal. The usual approach to the problem is to inscribe geometric shapes in the structure that represent the space where accommodation, easy diffusion, and free access for the guest species are expected. Such shapes are illustrated in Figure 3. One more problem arises from the static and average character of the structural model derived from XRD. The model does not account for the dynamics of the host framework, the presence of defects, and local distortions. These factors are especially important for flexible host frameworks whose structure will adapt as guests enter the pores.[1,2,19,51,52]

In this work, various approaches were tried to find an adequate but still simple calculation procedure. The scheme is

(45) Kitaigorodskii, A. I. *Molecular Crystals and Molecules*; Academic Press: New York, 1973.
(46) (a) Breck, D. W. *Zeolite Molecular Sieves*; Wiley: New York, 1974; Chapter 5, Section I, pp 425−438. (b) Breck, D. W. *Zeolite Molecular Sieves*; Wiley: New York, 1974; Chapter 8, Section C, pp 633−645.
(47) Voogd, P.; Scholten, J. J. F.; van Bekkum, H. *Colloids Surf.* **1991**, *55*, 163−171.
(48) Pires, J.; Carvalho, A.; Veloso, P.; de Carvalho, B. *J. Mater. Chem.* **2002**, *12*, 3100−3104.
(49) Ribeiro Carrott, M. M. L.; Russo, P. A.; Carvalhal, C.; Carrott, P. J. M.; Marques, J. P.; Lopes, J. M.; Gener, I.; Guisnet, M.; Ramôa Ribeiro, F. *Micropor. Mesopor. Mater.* **2005**, *81*, 259−267.
(50) Molinard, A.; Vansant, E. F. *Adsorption* **1995**, *1*, 49−59.
(51) Ratcliffe, C. I.; Soldatov, D. V.; Ripmeester, J. A. *Micropor. Mesopor. Mater.* **2004**, *73*, 71−79.
(52) Soldatov, D. V.; Enright, G. D.; Ripmeester, J. A. *Cryst. Growth Des.* **2004**, *4*, 1185−1194.

***Table 4.*** Channel Geometry in the Crystalline Dipeptides Studied[a]

| | experimental data | | | parameters calculated from crystal structure | | | | | |
|---|---|---|---|---|---|---|---|---|---|
| compound | $D^{(He)}$, Å | $\delta_{iso}$, ppm[b] | $\Delta\delta$, ppm [$\eta$][c] | $D_{av}$, Å | $D$ range, Å | helix radius, Å | full translation, Å | effective length per translation, Å | helicity |
| AV | 5.36(8) | 98.7 | 23.0 [0.15] | 5.014 | 4.98−5.05 | 0.60 | 10.027 | 10.71 | low |
| VA | 5.08(8) | 128.9 | 18.0 [0.10] | 4.724 | 4.63−4.77 | 1.13 | 10.083 | 12.32 | high |
| AI | 4.3(1) | 137.6 | 37.0 [0.05] | 4.740 | 4.66−4.78 | 0.58 | 10.221 | 10.85 | low |
| VV | 4.0(1) | 156.8 | 41.4 [0.05] | 4.390 | 4.26−4.48 | 0.57 | 10.354 | 10.95 | low |
| IA | 3.6(1) | 196.4 | 29.5 [0.10] | 3.736 | 3.70−3.76 | 1.01 | 10.037 | 11.88 | high |
| IV | 3.4(1) | 226.0 | 46.0 [0.05] | 3.904 | 3.85−3.93 | 0.92 | 10.305 | 11.80 | high |
| VI | 3.0(2) | 264.3 | 70.5 [0.00] | 3.702 | 3.66−3.75 | 0.32 | 10.319 | 10.51 | low |
| LS | 4.3(2) | 170.7 | 37.5 [0.05] | 4.930 | 4.90−4.96 | 0.12 | 6.163 | 6.21 | low |

[a] Experimental data and parameters calculated from crystal structure. [b] The reported values for $\delta_{iso}$ are from MAS experiments [c] Anisotropy $\Delta\delta$ and the asymmetry parameter $\eta$ are defined as follows: $\Delta\delta = \delta_{33} - \delta_{iso}$; $\eta = (\delta_{11} - \delta_{22})/(\delta_{33} - \delta_{iso})$; $\delta_{iso} = 1/3(\delta_{11} + \delta_{22} + \delta_{33})$, where $|\delta_{33} - \delta_{iso}| \geq |\delta_{11} - \delta_{iso}| \geq |\delta_{22} - \delta_{iso}|$.

briefly illustrated here for AV. *Experiment:* The porosity found from He pycnometry ($P^{(He)}$) was 12.5(2)%. The experimental porosity with respect to Xe ($P^{(Xe)}$) can be estimated from the limiting composition of AV*0.5Xe (three Xe atoms per unit cell) found in our previous work.[22] The volume the same quantity of Xe can occupy outside the pores may be found by taking the volume of the Xe atom as 42.2 Å$^3$ and assuming the limits of the packing efficiency for Xe atoms to be 74.05% (close packing) and 60% (a low limit for packing efficiency in van der Waals crystals).[45] From these considerations, the $P^{(Xe)}$ should be within 9.4−11.6%. *Calculations*: The calculation of "porosity" using the program ATOMS[43] (grid: 0.02 Å; sphere radius: 0.01 Å) yielded the value of 47% that actually represents the total empty space in the structure (see Table 3). Increasing the radius of the inscribed sphere to 1.40 Å (van der Waals radius of He) yielded the value of "porosity" of 4%. Program PLATON[53] yielded "porosity" of 17.3%. Our own calculation based on the program CLAT[13] sought the volume in the structure accessible to a sphere of 1.40 Å radius and yielded the value of 17.1%. Finally, only the method described in the Experimental section yielded a value of 10.90%, realistic and consistent with the experiment.

**Channel Size.** Experimental data and parameters derived from crystal structure that characterize the geometry of channels are summarized in Table 4.

As seen from He pycnometry, the average diameter of the channel ranges from 5.4 Å for AV to 3.0 Å for VI in the descending order given in Table 4. The eighth dipeptide LS, having a different structural type, reveals an intermediate channel diameter similar to that in AI.

The values derived from crystal structures follow basically the same trend although some distinctions are evident. The channel diameters for AV and VA seem to be underestimated. For this part, it should be kept in mind that the method used in the calculations does not refer to any specific guest molecule. For example, following the logic given in the previous section, the experimentally observed channel diameter in AV with respect to Xe would be from 4.65 to 5.16 Å, in good correspondence with the value of 5.014 Å calculated from the crystal structure. Another argument for the observed differences might be that the method used for calculation is rather simple and may not account for niches and other features of the channel geometry. Indeed, noticeably divergent results from He pycnometry and from crystal structure data for the VA-AI pair may be due to an essentially different geometry of channels in these two dipeptides (Figure 3). Our attempts to move calculations to a higher degree of precision revealed that the calculated dimensions of the channel dramatically change upon rotation of the methyl groups and other fragments and, therefore, should be used only as a first approximation to the understanding of the geometry and other properties of micropores.

The lowest values of the channel diameter obtained from He pycnometry are significantly smaller as compared to those calculated from XRD results and may be underestimated because not all of the pores in the actual sample are accessible to the He gas. Despite the stability of results upon variation of experimental conditions (see Experimental section), the blocking of very narrow channels in VI and other dipeptides cannot be excluded. The concentration of blocking sites may be similar from sample to sample due to either an equilibrium or reproducibly formed concentration of defects in the crystal structure.[54] In particular, the problem of blocking narrow isolated pores is known for zeolites.[55−58] On the other hand, the diffusion of He atoms may be limited by the diffusion of trace impurities available in the channels (including clusters of water or products of dipeptide degradation) as well as by the dynamics of the host matrix itself. It was well demonstrated that for pores based on polypeptides, such as gramicidin,[59] lysozyme,[23] and $\beta$−lactoglobulin,[4] the diffusion of guest is a part of a concerted process where the flexible host matrix is an active participant. Indeed, it is quite evident from this work that pores in at least three of the materials studied were hardly accessible for Xe if their host structure was rigid.

Solid-state $^{129}$Xe NMR is quite established as an informative method to study void spaces in materials.[60−66] All materials

(53) Spek, A. L. *J. Appl. Crystallogr.* **2003**, *36*, 7−13.
(54) Newsam, J. M.; Deem, M. W. *J. Phys. Chem.* **1995**, *99*, 8379−8381.
(55) Barrer, R. M.; Rees, L. V. *Trans. Faraday Soc.* **1954**, *50*, 989−999.
(56) Rees, L. V. C.; Berry, T. Sorption of Nonpolar Sorbates in Linde Sieve-A Modified by the Pre-sorption of Ammonia. In *Proceedings of Conf. on Molecular Sieves*; Soc. Chem. Ind.: London, 1967; pp 149−163.
(57) Silva, J. M.; Ribeiro, M. F.; Ribeiro, F. R.; Benazzi, E.; Gnep, N. S.; Guisnet, M. *Zeolites* **1996**, *16*, 275−280.
(58) Skoulidas, A. I.; Sholl, D. S. *J. Phys. Chem. A* **2003**, *107*, 10132−10141, and refs 1−3 therein.
(59) Turano, B.; Pear, M.; Busath, D. *Biophys. J.* **1992**, *63*, 152−161.
(60) Ripmeester, J. A.; Ratcliffe, C. I.; Tse; J. S. *J. Chem. Soc., Faraday Trans. 1* **1988**, *84*, 3731−3745.
(61) Ripmeester J. A.; Ratcliffe, C. I. *J. Phys. Chem.* **1990**, *94*, 7652−7656.
(62) Terskikh, V. V.; Mudrakovskii, I. L.; Mastikhin, V. M. *J. Chem. Soc., Faraday Trans.* **1993**, *89*, 4239−4243.
(63) Ripmeester, J. A.; Ratcliffe, C. I. *Energy Fuels* **1998**, *12*, 197−200.
(64) Bonardet, J. L.; Fraissard, J.; Gédéon, A.; Springuel-Huet, M. A. *Catal. Rev.-Sci. Eng.* **1999**, *41*, 115−225.
(65) Terskikh, V. V.; Moudrakovskii, I. L.; Breeze, S. R.; Lang, S.; Ratcliffe, C. I.; Ripmeester, J. A.; Sayari, A. *Langmuir* **2002**, *18*, 5653−5656.
(66) Stueber, D.; Jameson, C. J. *J. Chem. Phys.* **2004**, *120*, 1560−1571.

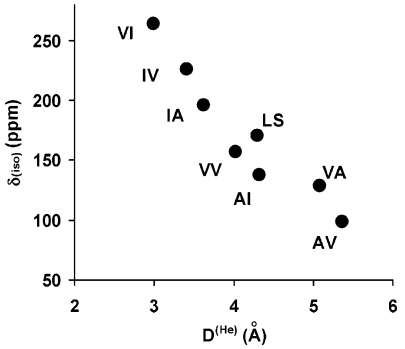


***Figure 4.*** Correlation between isotropic shift $\delta_{iso}$ ($^{129}$Xe NMR experiment) and experimental diameter of the channel $D^{(He)}$ (He pycnometry) for the studied series.

studied revealed strong static $^{129}$Xe NMR spectra of xenon adsorbed in the channels with prominent anisotropy of the chemical shift and nearly axial line shapes with $\eta \approx 0$ (Table 4). One needs to note that because the Xe−$N_2$−He mixture used in these experiments contains only 1% of xenon (a partial pressure of only 10 mbar), the spectra correspond to very low Xe loadings and a situation where Xe−Xe interactions are negligible. Such experimental conditions ensure that the main contributing factor in the spectra originates from interaction of the xenon atom with the channels. The observed line shapes are in a very good agreement with those expected for the cylindrical or nearly cylindrical nano-channels.[67,68] The span of observed anisotropies is consistent with both the size and general geometry of the pores.[15,33,34,67−69]

For families of chemically similar materials, simple correlations were found between the size of cavities available for guest inclusion and the isotropic chemical shift of the Xe atom included in the cavity.[29,60−63,65,66] In this work, a good correspondence was observed between the value of the diameter obtained from He pycnometry and the isotropic shift of $^{129}$Xe ($\delta_{iso}$) included in the channels (Table 4 and Figure 4). It should be noted that He pycnometry works as an integral method, making it possible to extract the total quantity of pore space in the materials, whereas $^{129}$Xe NMR is a local method providing information on pore geometry on a molecular-level scale. The correspondence of the two independent experimental methods is substantial and strongly supports the validity of the results obtained.

Similar to numerous empirical correlations between $^{129}$Xe isotropic chemical shift and the pore size,[60−65,70] the dependence shown in Figure 4 demonstrates close-to-parabolic dependence. As known from the clathrate hydrate cages,[60,61,67,68] the dimension of the channel is the main factor affecting the isotropic chemical shift of adsorbed xenon. Despite the pronounced difference in channels chiralities of the dipeptides studied, as will be discussed later, only minor deviations from the general trend are observed for the isotropic chemical shift values.

Compiling the results of the three methods used in this study, the following order for the channel diameter may be established:

$$\mathrm{AV} > \underbrace{\mathrm{VA} > \mathrm{AI} > \mathrm{VV}}_{\mathrm{LS}} > \mathrm{IA} > \mathrm{IV} > \mathrm{VI}$$

This order accounts for both static and dynamic components of the channel cross-section and is expected to be valid for the majority of guest molecules of small size and simple geometry. The eighth dipeptide LS can only approximately be placed in the series as its structure and the channel organization are appreciably different.

According to IUPAC recommendations,[71] the 3−5 Å pores in the materials of this work should be classified as micropores. The observed dimensions come near the lowest size limit of any pores taken as 2.6 Å, the kinetic diameter of the smallest gas molecule He.[46b] Pores of this size are frequently referred as "ultramicropores" (although the term is not supported by IUPAC).[72] The greatest interest in ultramicroporous materials is their application in gas separation technologies exploiting either a sorption−diffusion mechanism in membranes[73−77] or pressure/temperature swing adsorption.[78,79]

We note the presence of Xe in channels that appear to be rather smaller than the Xe van der Waals diameter (4.3 Å) as judged from the probing of the channels with He. As pointed out, the channels, in fact, may be larger when the Xe guests are present, thus drawing attention both to the flexibility of the framework and to the role of cooperative dynamics in allowing the first Xe atoms to enter the channels, as no significant kinetic barriers were noted during the sorption experiments.

**Channel Shape and Helicity.** The channels in all dipeptides studied are very uniform, with the variation of diameter as the channel propagates along *c* translation being 0.2 Å or less (Table 4). Such geometry is very uncommon among inclusion architectures and is reminiscent of the channel in urea.[14,18,22] The cylindrical shape of the urea channel accounts for the formation of incommensurate host−guest phases,[80] whose fascinating physical properties continue to attract ever-increasing attention.[81−86]

However, there is a significant distinction of the channel in the dipeptides studied. Unlike for urea, the center of the channel is displaced from the central axis by up to >1 Å (Table 4). Due to the channel symmetry of $6_1$ ($6_5$ for LS) there are six

(67) Ripmeester, J. A. *J. Am. Chem. Soc.* **1982**, *104*, 289−290.
(68) Jameson, C. J.; de Dios, A. C. *J. Chem. Phys.* **2002**, *116*, 3805−3821.
(69) Ripmeester, J. A.; Ratcliffe, C. I. **1995** *J. Phys. Chem. 99*, 619
(70) Demarquay, J.; Fraissard, J. *Chem. Phys. Lett.* **1987**, *136*, 314−318;
(71) Rouquerol, J.; Avnir, D.; Fairbridge, C. W.; Everett, D. H.; Haynes, J. H.; Pernicone, N.; Ramsay, J. D. F.; Sing, K. S. W.; Unger, K. K. *Pure Appl. Chem.* **1994**, *66*, 1739−1758, and refs 1, 3, 4 therein.
(72) Sing, K. S. W.; Everett, D. H.; Haul, R. A. W.; Moscou, L.; Pierotti, R. A.; Rouquerol, J.; Siemieniewska, T. *Pure Appl. Chem.* **1985**, *57*, 603−619.
(73) Jones, C. W.; Koros, W. J. *Carbon* **1994**, *32*, 1419−1425.
(74) Tsai, C.-Y.; Tam, S.-Y.; Lu, Y.; Brinker, C. J. *J. Membr. Sci.* **2000**, *169*, 255−268.
(75) Da Costa, J. C. D.; Lu, G. Q.; Rudolph, V. *J. Nanosci. Nanotechnol.* **2004**, *4*, 265−269.
(76) Kreisberg, V. A.; Rakcheev, V. P.; Antropova, T. V. *J. Porous Mater.* **2005**, *12*, 13−22.
(77) Steel, K. M.; Koros, W. J. *Carbon* **2005**, *43*, 1843−1856, and ref 1 therein.
(78) Ko, D.; Siriwardane, R.; Biegler, L. T. *Ind. Eng. Chem. Res.* **2003**, *42*, 339−348, and refs 1−3 therein.
(79) Yamamoto, T.; Endo, A.; Ohmori, T.; Nakaiwa, M.; Mukai, S. R.; Tamon, H. *Drying Technol.* **2005**, *23*, 2119−2129, and ref 10 therein.
(80) Hollingsworth, M. D.; Harris, K. D. M. Urea, Thiourea and Selenourea. In *Comprehensive Supramolecular Chemistry*; Atwood, J. L., Davies, J. E. D., MacNicol, D. D., Vögtle, F., Eds.; Pergamon: Oxford, 1996; Vol. 6, pp 177−237.
(81) Brown, M. E.; Hollingsworth, M. D. *Nature* **1995**, *376*, 323−327.
(82) Currat R. *Ferroelectrics* **2000**, *236*, 11−22.
(83) Le Lann, H.; Toudic, B.; Lefont, R.; Etrillard, J.; Guillaume, F.; Rufflé, B.; Ollivier, J.; Lechner, R. E.; Breczewski, T. *Physica B (Amsterdam)* **2000**, *276−278*, 298−299.
(84) Lefort, R.; Toudic, B.; Etrillard, J.; Guillaume, F.; Bourges, P.; Currat, R.; Breczewski, T. *Eur. Phys. J. B* **2001**, *24*, 51−57.
(85) Krieger, J. H.; Semenov, A. R.; Chekhova, G. N. *Phys. Solid State* **2001**, *43*, 2060−2062.
(86) Yeo, L.; Harris, K. D. M. *Mendeleev Commun.* **2004**, 263−266, and ref 14 therein.

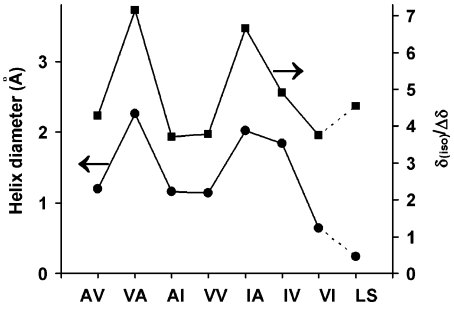


***Figure 5.*** The correlation between the diameter of a helix drawn in the channel (calculated from crystal structure, ●) and $\delta_{iso}/\Delta\delta$ ratio (derived from $^{129}$Xe NMR experiment, ■) for the series studied. The connecting lines serve illustrative purposes.

equivalent sites along a translation, turned by 60° and shifted by 1/6 of the translation, or ∼1.7 Å (∼1 Å for LS). This organization results in the helicity of the channel: its center crawls around the central axis (Figure 3).

The helicity of a channel may be described in terms of parameters of the helix that follow the center of the channel at each point along the channel. There are three such parameters: radius (diameter), pitch, and handedness of the helix. In our case, the radius is the deviation of the center of the channel from the $6_1$ axis, average of values taken on different levels (Table 4). The pitch is equal to a full translation along the channel (Table 4), that is, to the *c* crystallographic parameter. Finally, the handedness is right for the seven dipeptides crystallizing in $P6_1$ space group but left for LS crystallizing in $P6_5$.

The consequences of the helicity are the presence of a perpendicular component and the pronounced chirality of the pore space. The presence of the perpendicular component is important because it results in the effective elongation of the channel by up to 22% (Table 4). The comparison of AV and VA shows that although the former gains in the channel diameter, the latter may have a higher capacity for certain guest species: due to helicity, its channel effectively has an additional 1.6 Å per translation.

The presence of helicity in the channels is well sensed by $^{129}$Xe NMR. Using the principles suggested and developed for the shape of the adsorption site,[67−69] one can expect that for the same size of channel, the presence of helicity should lead to reduced magnitudes of anisotropy due to a lesser difference between the parallel and perpendicular components in the shielding tensor of adsorbed xenon. As a demonstration of very high sensitivity of the $^{129}$Xe anisotropy to the channels geometry, a correlation between calculated helix diameter and the $\delta_{iso}/\Delta\delta$ ratio derived from NMR experiment is shown in Figure 5. One should note that on this graph, the anisotropy is effectively normalized to the size of the channel through the isotropic shift; thus, the effect of the channel size on $\Delta\delta$ is practically excluded.

On the basis of the results of this work, the following order for the channel helicity may be established:

$$\underbrace{\mathrm{VA} > \mathrm{IA} > \mathrm{IV}}_{\text{high}} > \underbrace{\mathrm{AV} \sim \mathrm{AI} \sim \mathrm{VV} > \mathrm{VI} > \mathrm{LS}}_{\text{low}}$$

The first three, VA, IA, and IV, have a high helicity with the diameter of the helix ∼2 Å. The remaining five will be taken as having low helicity with the diameter of the helix ∼1 Å or less. The qualitative difference is apparent from Figure 3, which compares the channel geometry of the eight dipeptides.

The chirality of microporous space in the materials studied may be prospective for chiral recognition or separation. The introduction of chirality in microporous materials is one of the topical tasks in crystal engineering, with significant efforts having been made.[87,88] At the same time, the lower peptides, as those of the present study, may form a new family of naturally, intrinsically chiral sorbent materials.

**Comparison with Other Materials.** Supramolecular structures based on lower peptides may be subdivided into two groups: peptide nanotubes and peptide clathrates. Peptide nanotubes, known from the pioneering studies of Ghadiri and co-workers,[89] have attracted a significant research effort.[90−94] Peptide clathrates are crystalline materials comprising guest components in a peptide matrix.[95−101] The crystalline dipeptides studied in this work represent a somewhat intermediate position exhibiting peptide nanotubes organized inside a crystal matrix.

On the topology of void space (open 1D channels), the materials studied and their inclusion products should be classified as tubulands and tubulates, respectively.[102] A brief comparison with urea was given in the previous section and in our earlier work.[22]

On the stability of the host framework, the dipeptides studied are sorbents as their micropore architecture is stable in the absence of guest species. The expected inclusion behavior of such materials is sorption (as opposed to clathration, encapsulation, and dissolution),[2] with a variable guest-to-host ratio.[103] A distinction from currently used sorbents is the flexibility of the dipeptide matrix that makes the act of sorption a dynamic process where the host matrix may respond individually to the presence of each particular guest.[2,104] In particular, the transformations of AV and LS matrixes, including the formation of a superlattice and anisotropic expansion, were reported by Görbitz.[25,28] One of the potential applications for the new

(87) Lin, W. *J. Solid State Chem.* **2005**, *178*, 2486-2490.
(88) Bradshaw, D.; Claridge, J. B.; Cussen, E. J.; Prior, T. J.; Rosseinsky, M. J. *Acc. Chem. Res.* **2005**, *38*, 273−282.
(89) Ghadiri, M. R.; Granja, J. R.; Milligan, R. A.; McRee, D. E.; Khazanovich, N. *Nature* **1993**, *366*, 324−327.
(90) Hartgerink, J. D.; Clark, T. D.; Ghadiri, M. R. *Chem.−Eur. J.* **1998**, *4*, 1367−1372.
(91) Bong, D. T.; Clark, T. D.; Granja, J. R.; Ghadiri, M. R. *Angew. Chem., Int. Ed.* **2001**, *40*, 988−1011.
(92) Görbitz, C. H. Peptide Nanotubes. In *Encyclopedia of Supramolecular Chemistry*; Atwood, J. L., Steed, J. W., Eds.; Marcel Dekker: New York, 2004; pp 1305−1341.
(93) Reches, M.; Gazit, E. *Israel J. Chem.* **2005**, *45*, 363−371.
(94) Gao, X.; Matsui, H. *Adv. Mater.* **2005**, *17*, 2037−2050.
(95) Pavone, V.; Benedetti, E.; Di Blasio, B.; Lombardi, A.; Pedone, C.; Tomasich, L.; Lorenzi, G. P. *Biopolymers* **1989**, *28*, 215−223.
(96) Görbitz, C. H. *Acta Crystallogr., Sect. C: Cryst. Struct. Commun.* **1999**, *55*, 2171−2177.
(97) Hušák, M.; Kratochvíl, B.; Císařová, I.; Jegorov, A. *Collect. Czech. Chem. Commun.* **2000**, *65*, 1950−1958.
(98) Jegorov, A.; Pakhomova, S.; Hušák, M.; Kratochvíl, B.; Žák, Z.; Cvak, L.; Buchta, M. *J. Inclusion Phenom.* **2000**, *37*, 137−153.
(99) Jegorov, A.; Hušák, M.; Kratochvíl, B.; Císařová, I. *Cryst. Growth Des.* **2003**, *3*, 441−444.
(100) Akazome, M.; Hirabayashi, A.; Ogura, K. *Tetrahedron* **2004**, *60*, 12085−12093, and refs 5−7 therein.
(101) Akazome, M.; Hirabayashi, A.; Takaoka, K.; Nomura, S.; Ogura, K. *Tetrahedron* **2005**, *61*, 1107−1113, and refs 4, 8, 9 therein.
(102) Weber, E. Classification and Nomenclature of Supramolecular Compounds. In *Encyclopedia of Supramolecular Chemistry*; Atwood, J. L., Steed, J. W., Eds.; Marcel Dekker: New York, 2004; pp 261−273.
(103) Belosludov V. R.; Lavrentiev M. Y.; Dyadin Y. A. *J. Inclusion Phenom.* **1991**, *10*, 399−422.
(104) Soldatov, D. V. Stimuli-responsive Supramolecular Solids: Functional Porous and Inclusion Materials. In *Stimuli-responsive Polymeric Films and Coatings*; Urban, M. W., Ed.; American Chemical Society: Washington, 2005; Chapter 13, pp 214−231.

sorbents may be the sorption of gases for separation, purification, storage, or other purposes. Sorbents with narrow pores are attractive for highly volatile species and are superior to materials with giant pores.[105,106]

A prominent distinction of the peptide hosts studied is their natural, biological origin. Surprisingly, very few organically based host materials are known that are based on natural, or closely related to natural, building elements: urea,[80] cyclodextrins,[107] amylose,[108−110] gossypol,[111] bile acids,[112] and porphyrins.[113] As a rule, such hosts become objects of extensive, ever-increasing studies in various fields, from physics and biology to food industry and medicine. Cyclodextrins are especially representative of a success story being widely utilized in various industries.[114−117] On the other hand, new natural hosts are rarely found, as opposed to the remarkable progress in the development of synthetic host materials.

The helical structure of the dipeptides studied may serve as a simple, very well-defined model for trans-membrane channels and pores. The peptide helix is a dominating motif in ion channels,[118] aquaporins,[119] and peptide structures of various receptors, antimicrobial agents, and antibiotics.[120−125] Unmodified dipeptides are the simplest peptide molecules, and the presence of properties similar to those of biologically relevant higher peptides and proteins should not be overlooked.

Further advantages of the dipeptides studied might be foreseen for practical applications in biological and medical contexts. The dipeptides are harmless, biocompatible, and environmentally friendly. The cost of their production can be reduced substantially with aspartame, a worldwide used dipeptide derivative, as precedent.[126] The potential diversity of peptide sorbents and host materials, resulting from the multitude of both amino acids and their combinations, is tremendous and is still to be explored in greater depth soon.

## List of Abbreviations

AV − L-Alanyl-L-Valine
VA − L-Valyl-L-Alanine
AI − L-Alanyl-L-Isoleucine
VV − L-Valyl-L-Valine
IA − L-Isoleucyl-L-Alanine
IV − L-Isoleucyl-L-Valine
VI − L-Valyl-L-Isoleucine
LS − L-Leucyl-L-Serine
CF − continuous flow
$d_{calc}$ − density calculated from XRD data (room temperature)
$d^{(He)}$ − density determined with He pycnometry (density of the host body framework, "skeletal density")
$D_{av}$ − average channel diameter from crystal structure data
$D^{(He)}$ − average diameter of the channel calculated from He pycnometry results
HP Xe − hyperpolarized xenon
$k_{pack}$ − packing coefficient
MAS − magic angle spinning
$P^{(He)}$ − total porosity in a material calculated by the comparison of $d^{(He)}$ and $d_{calc}$
$P^{(Xe)}$ − total porosity with respect to Xe
$V_{empty}$ − volume of unit cell accessible to He (micropore space per unit cell)
$V_{u.cell}$ − volume of the unit cell
$\delta_{iso}$ − isotropic shift in $^{129}$Xe solid-state NMR; $\delta_{iso} = 1/3(\delta_{11} + \delta_{22} + \delta_{33})$, with $\delta_{11}$, $\delta_{22}$, $\delta_{33}$ being the principal components of the chemical shift tensor
$\Delta\delta$ − anisotropy in $^{129}$Xe solid-state NMR defined as $\Delta\delta = \delta_{33} - \delta_{iso}$, with $|\delta_{33} - \delta_{iso}| \geq |\delta_{11} - \delta_{iso}| \geq |\delta_{22} - \delta_{iso}|$
$\eta$ − asymmetry parameter in $^{129}$Xe solid-state NMR; $\eta = (\delta_{11} - \delta_{22})/(\delta_{33} - \delta_{iso})$

**Acknowledgment.** D.V.S. acknowledges support of the research on microporous dipeptides at the Steacie Institute for Molecular Sciences, National Research Council Canada. Furthermore, the assistance of S. Lang (He pycnometry), G. D. Enright (crystallography), and K. A. Udachin (ATOMS) from the Institute is greatly appreciated.

**Supporting Information Available:** CIF files of six structures studied in this work (see Table 1) are available. This material is available free of charge via the Internet at http://pubs.acs.org.

JA060474J

(105) Pan, L.; Sander, M. B.; Huang, X.; Li, J.; Smith, M.; Bittner, E.; Bockrath, B.; Johnson, J. K. *J. Am. Chem. Soc.* **2004**, *126*, 1308−1309.
(106) Kaye, S. S.; Long, J. R. *J. Am. Chem. Soc.* **2005**, *127*, 6506−6507.
(107) Cyclodextrins. In *Comprehensive Supramolecular Chemistry*; Atwood, J. L., Davies, J. E. D., MacNicol, D. D., Vögtle, F., Eds.; Pergamon: Oxford, 1996; Vol. 3.
(108) Kubik, S.; Höller, O.; Steinert, A.; Tolksdorf, M.; Wulff, G. *Macromol. Symp.* **1995**, *99*, 93−102, and refs 18−20 therein.
(109) Kadokawa, J.; Nakaya, A.; Kaneko, Y.; Tagaya, H. *Macromol. Chem. Phys.* **2003**, *204*, 1451−1457, and refs 4, 5, 7, 8 therein.
(110) Wulff, G.; Avgenaki, G.; Guzmann, M. S. P. *J. Cereal Sci.* **2005**, *41*, 239−249, and refs therein.
(111) Ibragimov, B. T.; Talipov, S. A. *J. Struct. Chem.* **1999**, *40*, 686−704.
(112) Kato, K.; Inoue, K.; Tohnai, N.; Miyata, M. *J. Inclusion Phenom.* **2004**, *48*, 61−67, and ref 1 therein.
(113) Goldberg, I. *Chem. Commun.* **2005**, 1243−1254, and refs therein.
(114) Szejtli, J. Cyclodextrin Technology; Kluwer: Dordrecht, 1988.
(115) Hedges, A. R. *Chem. Rev.* **1998**, *98*, 2035−2044.
(116) Uekama, K.; Hirayama, F.; Irie, T. *Chem. Rev.* **1998**, *98*, 2045−2076.
(117) Hashimoto, H. *J. Inclusion Phenom.* **2002**, *44*, 57−62.
(118) MacKinnon, R. *Angew. Chem., Int. Ed.* **2004**, *43*, 4265−4277.
(119) Agre, P. *Angew. Chem., Int. Ed.* **2004**, *43*, 4278−4290.
(120) Balaram, P.; Krishna, K.; Sukumar, M.; Mellor, I. R.; Sansom, M. S. P. *Eur. Biophys. J.* **1992**, *21*, 117−128.
(121) Shai, Y. *Biochim. Biophys. Acta* **1999**, *1462*, 55−70.
(122) Dathe, M.; Wieprecht, T. *Biochim. Biophys. Acta* **1999**, *1462*, 71−87.
(123) Law, R. J.; Forrest, L. R.; Ranatunga, K. M.; La Rocca, P.; Tieleman, D. P.; Sansom, M. S. P. *Proteins* **2000**, *39*, 47−55.
(124) Futaki, S.; Fukuda, M.; Omote, M.; Yamauchi, K.; Yagami, T.; Niwa, M.; Sugiura, Y. *J. Am. Chem. Soc.* **2001**, *123*, 12127−12134.
(125) Andersen, O. A.; Koeppe, R. E., II; Roux, B. *IEEE Trans. Nanobiosci.* **2005**, *4*, 10−20.
(126) Mazur, R. Sweeteners. In *Encyclopedia of Chemical Technology*; Mark, H. F., Othmer, D. F., Overberger, C. G., Seaborg, G. T., Eds.; Wiley: New York, 1983; Vol. 22, pp 448−464.